

Sensing Based on Quantum Correlation of Photons in the Weak Nonlinear Regime

Zi-Qiang Yin,¹ Zhi-Hao Liu,¹ Jian Tang,¹ Hui Jing,^{1,2} and Xun-Wei Xu^{1,2,*}

¹*Key Laboratory of Low-Dimensional Quantum Structures and Quantum Control of Ministry of Education, Key Laboratory for Matter Microstructure and Function of Hunan Province, Department of Physics and Synergetic Innovation Center for Quantum Effects and Applications, Hunan Normal University, Changsha 410081, China*

²*Institute of Interdisciplinary Studies, Hunan Normal University, Changsha, 410081, China*

(Dated: December 2, 2024)

Quantum correlation of photons based on quantum interference, such as unconventional photon blockade (UPB), has been extensively studied for realizing single-photon sources in weak nonlinear regime. However, how to use this effect for other practical applications is rarely studied. Here, we propose schemes to realize sensitive sensing by the quantum correlation of photons based on quantum interference. We demonstrate that UPB can be observed in the mixing field output from a Mach–Zehnder interferometer (MZI) with two cavities in the two arms based on quantum interference. We show that the second-order correlation function of the output field is sensitive to the parameters of system, and propose schemes to realize angular velocity and temperature sensing by measuring the second-order correlation of the photons output from the MZI. We find that the second-order correlation function of the output field is much more sensitive to the parameters of system than the mean photon number, which provides an application scenario for the quantum correlation of photons in sensitive sensing.

I. INTRODUCTION

Quantum correlation of photons can be described by the correlation functions [1, 2], which provide a quantitative quantity to characterize the quantum nature of lights. To date, the application of quantum photon correlation has been expanded from characterizing single photons [3, 4] to demonstrating photonic quantum logic gate [5, 6] and fractional quantum Hall state [7].

The quantum correlation of photons can be manipulated when they passing through an optical system containing strong photon-photon interaction. If the probabilities of multiphoton states are suppressed by the nonlinear interaction, then the output field becomes sub-Poissonian, which is referred as conventional photon blockade (CPB) [8]. CPB has been proposed in various optical platforms [9–20], and has been observed in the resonators strongly coupled to quantum emitters [21–27].

In the past decade, some novel mechanisms are proposed to manipulate the correlation properties of photons under weak nonlinear interactions [28–40]. The one that attracts the most attention is the unconventional photon blockade (UPB) [41, 42] that the probabilities of two-photon excitation is suppressed by destructive interference between different transition paths. UPB has been extensively studied in various systems, such as coupled optomechanical systems [43–45], coupled cavities with second or third order nonlinearities [46–60], cavity embedded with a quantum dot [61–65], coupled-resonator chain [66–68], etc. UPB has been experimentally realized with a quantum dot in the semiconductor cavity quantum electrodynamics system [69] and with a SQUID in superconducting resonators [70].

In a recent work, we found that the photon correlation of the mixing fields output from a Mach–Zehnder interferometer (MZI), with two cavities in the two arms, can be manipulated by quantum interference [71]. We uncover a scaling enhancement of photon blockade in the mixing fields output from the MZI. However, whether strong quantum correlation in the mixing output fields can also be realized in the weak nonlinear regime is still an open question. Moreover, we know that MZI [72] is a good platform for the measurement of the relative phase acquired by the beam along the two paths, which offers applications in versatile sensing based on the interference pattern [73–75]. How to use the photon correlation in the mixing fields output from MZI for sensing is another interesting question.

In this paper, we propose to realize sensitive sensing based on the correlation properties of mixing fields output from a MZI, with two cavities in the two arms based on weak nonlinearity. We find that strong photon blockade can be realized in the weak nonlinear regime by the quantum interference between different paths for two photons states passing through the MZI. We also show that the second-order correlation of the photons output from the MZI is sensitive to the system parameters, which is the main mechanism for sensing based on quantum correlation. As examples, we propose schemes to realize angular velocity sensing [76–87] and temperature sensing [88–115] by measuring the second-order correlation of the photons output from the MZI. Interestingly, the second-order correlation is much more sensitive to the parameters of system than the mean photon number, so that the sensing schemes by detecting second-order correlation may achieve a higher sensitivity than the schemes by measuring the mean photon number.

The paper is organized as follows. In Sec. II, we present the model of a MZI with two cavities in the two arms.

* xwxu@hunnu.edu.cn

We show UPB in the output field of the MZI both numerically and analytically in Sec. III. We demonstrate how to realize versatile sensing by measuring the second-order correlation of the photons output from the MZI in Sec. IV. Finally, we summary our main results in Sec. V.

II. PHYSICAL MODEL

We consider a MZI with two cavities (a_1 and a_2) in the two arms, as shown in Fig. 1(a). A laser is divided into two beams by a 50/50 beam splitter (BS), and then injected into one of the cavities, respectively. The output fields from these two cavities mix by another 50/50 BS, and a phase shifter (PS) is placed in one of the two paths. The second-order correlation of the mixing output field is measured by a Hanbury-Brown-Twiss (HB-T) set-up. In the frame rotating at the probe laser frequency ω_p , the system can be described by the Hamiltonian ($\hbar = 1$),

$$H = \Delta_1 a_1^\dagger a_1 + U a_1^\dagger a_1^\dagger a_1 a_1 + i\varepsilon (a_1^\dagger - a_1) + \Delta_2 a_2^\dagger a_2 + i\varepsilon (a_2^\dagger - a_2), \quad (1)$$

where a_i and a_i^\dagger are the annihilation and creation operators of the cavity mode i with resonance frequency ω_i ($i = 1, 2$), $\Delta_i = \omega_i - \omega_p$ is the detuning of the probe laser from the cavity resonance, $\delta = \omega_2 - \omega_1$ is the detuning between the two cavity modes, U is the nonlinear interaction strength in cavity 1, and ε is the driving strength on each cavity mode.

The two mixing fields a_{out} and A_{out} output from the MZI can be obtained according to the input-output relation [116], as

$$a_{\text{out}} = (\sqrt{\kappa_1} a_1 + e^{i\phi} \sqrt{\kappa_2} a_2) / \sqrt{2} - a_{\text{vac}} \quad (2)$$

and

$$A_{\text{out}} = (\sqrt{\kappa_1} a_1 - e^{i\phi} \sqrt{\kappa_2} a_2) / \sqrt{2} - a'_{\text{vac}}, \quad (3)$$

where κ_i is the decay rate from one of the cavity mirrors, ϕ is the relative phase between the output fields of the two arms (can be tuned by the phase shifter), and a_{vac} (a'_{vac}) is the input vacuum fields. As the output field A_{out} can be obtained from a_{out} just by replacing ϕ by $\phi + \pi$, we will only focus on the output field a_{out} in the following.

The quantum correlation of the output field a_{out} from the MZI can be described by the second-order correlation function

$$g_{\text{out}}^{(2)}(\tau) = \frac{\langle a_{\text{out}}^\dagger a_{\text{out}}^\dagger(\tau) a_{\text{out}}(\tau) a_{\text{out}} \rangle}{\langle a_{\text{out}}^\dagger a_{\text{out}} \rangle^2} \quad (4)$$

$$= \sum_{j,k,l,m=1}^2 e^{in\phi} \frac{\sqrt{\kappa_j \kappa_k \kappa_l \kappa_m} \langle a_j^\dagger a_k^\dagger(\tau) a_l(\tau) a_m \rangle}{4N_{\text{out}}^2},$$

where $n = l + m - j - k$, $2N_{\text{out}} = \kappa_1 \langle a_1^\dagger a_1 \rangle + \kappa_2 \langle a_2^\dagger a_2 \rangle + 2\sqrt{\kappa_1 \kappa_2} \text{Re}(e^{i\phi} \langle a_1^\dagger a_2 \rangle)$, and τ is the time delay between the two photodetectors (D_1 and D_2 in the HB-T set-up). There are cross-correlation between the photons in the two cavities (i.e., $\langle a_2^\dagger a_2 a_1^\dagger a_1 \rangle$, $\langle a_1^\dagger a_1^\dagger a_2 a_2 \rangle$, $\langle a_1^\dagger a_1^\dagger a_1 a_2 \rangle$, and $\langle a_2^\dagger a_1^\dagger a_2 a_2 \rangle$), and there are phase factors $e^{in\phi}$ in front of the terms, which can be negative and lead to the strong photon blockade in weak nonlinear regime based on quantum interference.

The system dynamics is governed by the master equation [117] for the density matrix ρ :

$$\frac{d\rho}{dt} = -i[H, \rho] + \sum_{i=1,2} \kappa_i \left(2a_i \rho a_i^\dagger - a_i^\dagger a_i \rho - \rho a_i^\dagger a_i \right), \quad (5)$$

In the following discussions, we will set $\kappa_1 = \kappa_2 = \kappa$ for simplicity, and the amplitude of the probe field is weak $\varepsilon = \kappa/10$.

III. PHOTON BLOCKADE WITH WEAK NONLINEARITY

First of all, let us discuss how to realize the photon blockade with weak nonlinearity in the MZI. The second-order correlation of the output field $\log_{10}[g_{\text{out}}^{(2)}(0)]$ is plotted as a function of the phase ϕ/π and detuning δ/κ for nonlinear strength $U/\kappa = 0.02$ in Fig 1(b). Strong photon anti-bunching $g_{\text{out}}^{(2)}(0) \ll 1$ is obtained around the parameters ($\delta \approx -0.47\kappa$, $\phi = 0.824\pi$) and ($\delta \approx 0.47\kappa$, $\phi = 1.104\pi$), with the weak nonlinearity ($U = 0.02\kappa$). The second-order correlation $\log_{10}[g_{\text{out}}^{(2)}(0)]$ is also plotted as a function of the nonlinear interaction strength U/κ and detuning δ/κ for $\phi = 0.824\pi$ in Fig 1(c). The minimal value of $\log_{10}[g_{\text{out}}^{(2)}(0)]$ is obtained around $U = 0.02\kappa$. The second-order correlation $g_{\text{out}}^{(2)}(\tau)$ versus time delay $\tau\kappa$ is shown in Fig 1(d). Different from the rapid oscillations induced by the coupling between two cavities predicted in weakly nonlinear photonic molecules [41, 42], here, there is no oscillation behavior as the delay time going on and the scale of the time delay is determined by the decay rate of the cavities as $1/\kappa$.

In order to understand the origin of the strong anti-bunching, we consider a non-Hermitian Hamiltonian including the decay effect as $H' = H - i\kappa_1 a_1^\dagger a_1 - i\kappa_2 a_2^\dagger a_2$, and use the wave function terminated to the two-photon states as

$$|\psi\rangle = C_{00}|0,0\rangle + C_{10}|1,0\rangle + C_{01}|0,1\rangle + C_{20}|2,0\rangle + C_{11}|1,1\rangle + C_{02}|0,2\rangle, \quad (6)$$

for weak probe fields $\varepsilon \ll \{\kappa_1, \kappa_2\}$. Substituting the non-Hermitian Hamiltonian and wave function into the Schrödinger's equation $i\hbar \frac{\partial}{\partial t} |\psi\rangle = H' |\psi\rangle$, we get the dynamical equations for the probability coefficients as

$$i \frac{d}{dt} C_{10} = (\Delta_1 - i\kappa_1) C_{10} + i\varepsilon C_{00}, \quad (7)$$

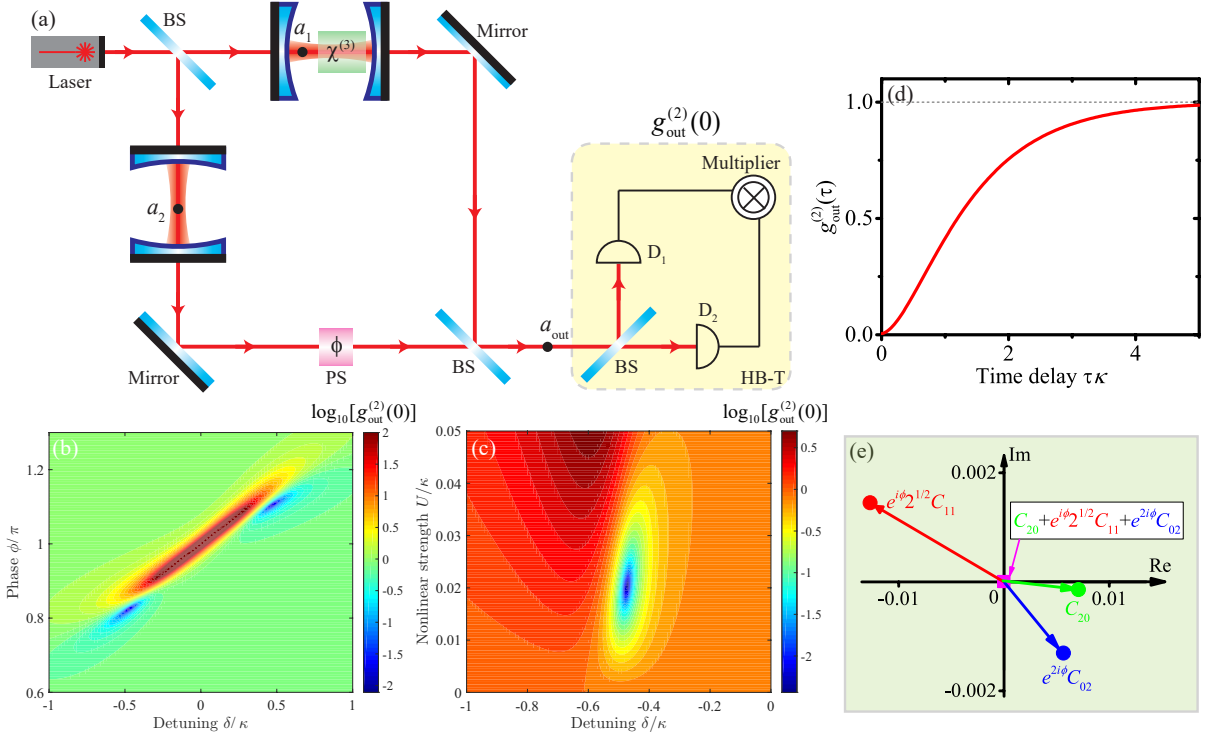


FIG. 1. (Color online) (a) A Mach-Zehnder interferometer with two cavities (a_1 and a_2) in the two arms. A laser is divided into two beams by a 50/50 beam splitter (BS), and then injected into one of the cavities, respectively. The output fields from these two cavities mix by another 50/50 BS, a phase shifter (PS) is placed in one of the two paths. The second-order fields of the output field is measured by a Hanbury-Brown-Twiss (HB-T) set-up. The second-order correlation $\log_{10}[g_{\text{out}}^{(2)}(0)]$ (b) versus phase ϕ/π and detuning δ/κ for nonlinear strength $U/\kappa = 0.02$, (c) versus U/κ and detuning δ/κ for $\phi = 0.824\pi$. (d) The second-order correlation $g_{\text{out}}^{(2)}(\tau)$ versus time delay $\tau\kappa$, and (e) the probability coefficients of two photons in the cavities (C_{20} , C_{11} , and C_{02}) and in the output field ($C_{20} + e^{i\phi}\sqrt{2}C_{11} + e^{2i\phi}C_{02}$), for $\delta \approx -0.47\kappa$, $\phi = 0.824\pi$, and $U/\kappa = 0.02$. The parameters are $\varepsilon/\kappa = 0.1$ and $\Delta_1 = 0$.

$$i \frac{d}{dt} C_{01} = (\Delta_2 - i\kappa_2) C_{01} + i\varepsilon C_{00}, \quad (8)$$

$$i \frac{d}{dt} C_{20} = (2\Delta_1 + 2U - i2\kappa_1) C_{20} + i\sqrt{2}\varepsilon C_{10}, \quad (9)$$

$$i \frac{d}{dt} C_{02} = (2\Delta_2 - i2\kappa_2) C_{02} + i\sqrt{2}\varepsilon C_{01}, \quad (10)$$

$$i \frac{d}{dt} C_{11} = (\Delta_1 + \Delta_2 - i\kappa_1 - i\kappa_2) C_{11} + i\varepsilon C_{10} + i\varepsilon C_{01}. \quad (11)$$

In the steady state, i.e., $dC_{ij}/dt = 0$, we have linear equations for the probability coefficients as

$$0 = (\Delta_1 - i\kappa_1) C_{10} + i\varepsilon C_{00}, \quad (12)$$

$$0 = (\Delta_2 - i\kappa_2) C_{01} + i\varepsilon C_{00}, \quad (13)$$

$$0 = (2\Delta_1 + 2U - i2\kappa_1) C_{20} + i\sqrt{2}\varepsilon C_{10}, \quad (14)$$

$$0 = (2\Delta_2 - i2\kappa_2) C_{02} + i\sqrt{2}\varepsilon C_{01}, \quad (15)$$

$$0 = (\Delta_1 + \Delta_2 - i\kappa_1 - i\kappa_2) C_{11} + i\varepsilon C_{10} + i\varepsilon C_{01}, \quad (16)$$

As $\varepsilon \ll \{\kappa_1, \kappa_2\}$, we assume that $C_{00} \approx 1 \gg \{|C_{10}|, |C_{01}|\} \gg \{|C_{20}|, |C_{02}|, |C_{11}|\}$, and under the conditions $\Delta_1 = 0$, $\Delta_2 = \delta$, $\kappa_1 = \kappa_2 = \kappa$, we get the expressions of the probability coefficients as

$$C_{10} = \frac{\varepsilon}{\kappa}, \quad (17)$$

$$C_{01} = \frac{-i\varepsilon}{\delta - i\kappa} \quad (18)$$

for single-photon states, and

$$C_{20} = \frac{-i}{U - i\kappa} \frac{\varepsilon^2}{\sqrt{2}\kappa}, \quad (19)$$

$$C_{02} = -\frac{1}{\sqrt{2}} \frac{\varepsilon^2}{(\delta - i\kappa)^2}, \quad (20)$$

$$C_{11} = -\frac{i\varepsilon^2}{\kappa(\delta - i\kappa)} \quad (21)$$

for two-photon states.

Based on the probability coefficients, the output photon intensity N_{out}/κ and second-order correlation function $g_{\text{out}}^{(2)}(0)$ can be expressed as

$$N_{R,\text{out}}/\kappa \approx \frac{1}{2} |C_{10} + e^{i\phi} C_{01}|^2, \quad (22)$$

and

$$g_{\text{out}}^{(2)}(0) \approx \frac{2 |C_{20} + \sqrt{2}e^{i\phi} C_{11} + e^{i2\phi} C_{02}|^2}{|C_{10} + e^{i\phi} C_{01}|^4}. \quad (23)$$

The optimal conditions for photon blockade is given by

$$C_{20} + \sqrt{2}e^{i\phi} C_{11} + e^{i2\phi} C_{02} = 0. \quad (24)$$

Under weak nonlinearity $U \ll \kappa$, the optimal conditions are obtained as

$$\frac{\delta_{\text{opt}}}{\kappa} \approx \pm \sqrt{\frac{\sqrt{2U/\kappa} - (U/\kappa)}{1 - \sqrt{2U/\kappa} + (U/\kappa)}}, \quad (25)$$

$$\phi_{\text{opt}} = \arg \left[- \left(1 + i \frac{\delta}{\kappa} \right) \left(1 - e^{i\frac{\pi}{4}} \sqrt{\frac{U}{\kappa}} \right) \right]. \quad (26)$$

The probability coefficients of two photons in the cavities (C_{20} , C_{11} , and C_{02}) and in the output field ($C_{20} + e^{i\phi}\sqrt{2}C_{11} + e^{i2\phi}C_{02}$) are shown in Fig 1(e) with the parameters ($\delta \approx -0.47\kappa$, $\phi = 0.824\pi$, $U/\kappa = 0.02$) for minimal of $g_{\text{out}}^{(2)}$, which agree well with Eqs. (24)-(26).

IV. QUANTUM SENSING BASED ON PHOTON BLOCKADE

We know that both of the output photon intensity N_{out}/κ and the second-order correlation function $g_{\text{out}}^{(2)}(0)$ depend on the parameters of the system, such as the phase ϕ and the detuning δ as shown in Fig. 2. From the figure, we can see that the phase interval $\Delta\phi$ from the maximum to minimum value of the second-order correlation function $g_{\text{out}}^{(2)}(0)$ is about $\Delta\phi \approx \pi/20$, which is much narrower than the phase interval ($\Delta\phi \approx \pi$) from the maximum to minimum value of the output photon intensity N_{out}/κ . The frequency interval $\Delta\omega$ from the maximum to minimum value of $g_{\text{out}}^{(2)}(0)$ is about $\Delta\omega \approx 0.18\kappa$, which is also much narrower than the frequency interval ($\Delta\omega \approx 2.4\kappa$) from the maximum to minimum value of N_{out}/κ . That is, the second-order correlation function $g_{\text{out}}^{(2)}(0)$ is much more sensitive to the parameters than the output photon intensity N_{out}/κ , which provides us a sensitive quantity for sensing. As examples, here we will propose two schemes to realize angular velocity sensing and temperature sensing, respectively, by measuring the second-order correlation of the photons output from the MZI.

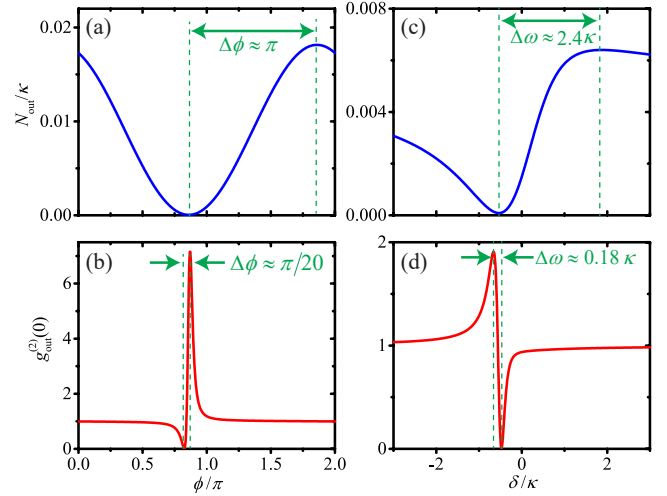


FIG. 2. (Color online) The output photon intensity N_{out}/κ and second-order correlation function $g_{\text{out}}^{(2)}(0)$, (a-b) versus phase ϕ/π with detuning $\delta/\kappa \approx -0.47$, and (c-d) versus δ/κ with $\phi = 0.824\pi$. The other parameters are the same as in Fig. 1(d).

A. Angular velocity sensing (gyroscope)

As a specific example, we consider the case that the platform rotates with an angular velocity Ω as shown in Fig. 3(a), which leads to an additional phase difference $\Delta\phi$ between the two beams as

$$\Delta\phi = \frac{4\pi A}{\lambda_0 c} \Omega, \quad (27)$$

where A is the area enclosed by the optical paths, λ_0 is wavelength of incident light, and c is the speed of light in vacuum. We set the phase difference $\phi_0 = 0.85\pi$ for the platform in the steady state, so we have the total phase difference $\phi = 0.85\pi + \Delta\phi$ for the system rotating with an angular velocity Ω . In the following numerical calculations, we take the parameters [118]: $A = 10^3 \text{ m}^2$ and $\lambda_0 = 1550 \text{ nm}$.

The output photon intensity N_{out}/κ and second-order correlation function $g_{\text{out}}^{(2)}(0)$ are plotted as functions of the angular velocity Ω in Fig. 3(b). We can see that the second-order correlation function $g_{\text{out}}^{(2)}(0)$ is much more sensitive to the change of the angular velocity Ω than the photon intensity N_{out}/κ . To characterize the sensitivity of N_{out}/κ and $g_{\text{out}}^{(2)}(0)$ to the change of the angular velocity Ω , we can define the sensitivity coefficients as

$$\eta_{n,\Omega} = \frac{dN_{\text{out}}/\kappa}{d\Omega}, \quad (28)$$

and

$$\eta_{g,\Omega} = \frac{dg_{\text{out}}^{(2)}(0)}{d\Omega}. \quad (29)$$

The sensitivities $\eta_{n,\Omega}$ and $\eta_{g,\Omega}$ are plotted as functions of the angular velocity Ω in Fig. 3(c). The maximal value of

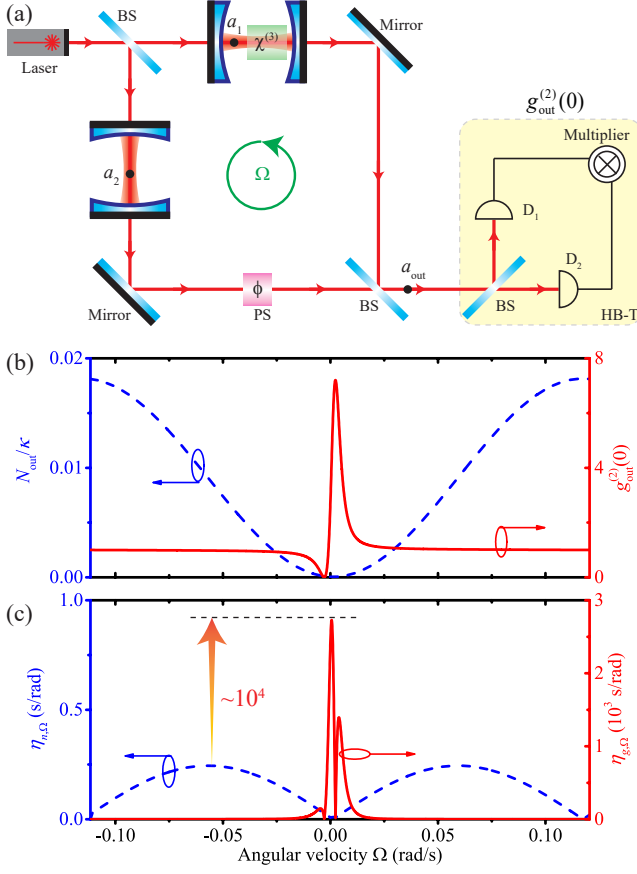


FIG. 3. (Color online) (a) The scheme to measure the angular frequency Ω . (b) The output photon intensity N_{out}/κ and second-order correlation function $g_{\text{out}}^{(2)}(0)$ versus Ω . (c) The sensitivities $\eta_{n,\Omega}$ and $\eta_{g,\Omega}$ versus Ω . The parameters are the same as in Fig. 1(d).

$\eta_{g,\Omega}$ is about four orders greater than the one of $\eta_{n,\Omega}$. It is known that the rotational angular velocity of the earth is about $\Omega_{\text{earth}} = 7.3 \times 10^{-5}$ rad/s, and we have $g_{\text{out}}^{(2)}(0) = 2.79$ for $\Omega = 0$ and $g_{\text{out}}^{(2)}(0) = 2.97$ for $\Omega = \Omega_{\text{earth}}$. Thus we can detect the rotation of the earth by measuring the second-order correlation function $g_{\text{out}}^{(2)}(0)$ of the photons output from the MZI.

B. Temperature sensing

In this subsection, we consider a dielectric layer in the cavity a_2 as shown in Fig. 4(a), and discuss how to measure the change of the temperature based on the thermal effect. Due to the thermal expansion, the thickness of the dielectric layer changes as

$$d(T) = d_0 (1 + \alpha \Delta T), \quad (30)$$

where d_0 is the thickness of the dielectric layer at a reference temperature, α is the thermal expansion coefficient, and ΔT is the variation of the temperature. In addition,

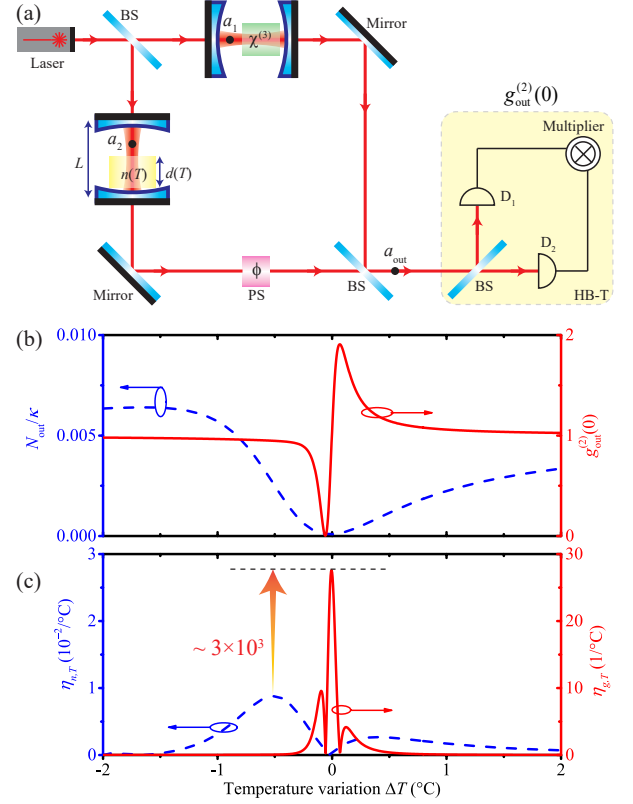


FIG. 4. (Color online) (a) The scheme to measure the temperature ΔT . (b) The output photon intensity N_{out}/κ and second-order correlation function $g_{\text{out}}^{(2)}(0)$ versus ΔT . (c) The sensitivities $\eta_{n,T}$ and $\eta_{g,T}$ versus ΔT . The parameters are the same as in Fig. 1(d).

as for the thermal-optical effect, the index of refraction also depends on the temperature as

$$n(T) = n_0 (1 + \beta \Delta T), \quad (31)$$

where n_0 is the index of refraction at a reference temperature and β is the thermal-optic coefficient. Based on these two factors, we have the frequency shift of the cavity a_2 is given approximately as

$$\delta_{\text{th}} \approx -\omega_2 \left[\frac{n_0 d_0}{L} \beta + \frac{(n_0 - 1) d_0}{L} \alpha \right] \Delta T, \quad (32)$$

where ω_2 the eigenfrequency of the cavity a_2 at a reference temperature with a cavity length L . Under the condition that $\omega_2 - \omega_1 = -0.56\kappa$, we have the detuning $\delta = -0.56\kappa + \delta_{\text{th}}$. As a simple example, we consider the dielectric layer as a SiO_2 layer, with the typical parameters [119, 120]: $\alpha = 5.5 \times 10^{-7}/^\circ\text{C}$, and $\beta = 1.0 \times 10^{-5}/^\circ\text{C}$, $n_0 = 1.45$ at the reference temperature 25°C , $\lambda_0 = 1550$ nm, $\omega_2 = 2\pi c/\lambda_0$, and $\omega_2/\kappa = 10^7$. The other parameters are $d_0 = 0.01$ mm and $L = 1$ mm.

The output photon intensity N_{out}/κ and second-order correlation function $g_{\text{out}}^{(2)}(0)$ are plotted as functions of temperature variation ΔT in Fig. 4(b). We can see

that the second-order correlation function $g_{\text{out}}^{(2)}(0)$ is much more sensitive to the variation of the temperature ΔT than the output photon intensity N_{out}/κ . To characterize the sensitivity of N_{out}/κ and $g_{\text{out}}^{(2)}(0)$ with respect to ΔT , we can define the sensitivity coefficients as

$$\eta_{n,T} = \frac{dN_{\text{out}}/\kappa}{dT}, \quad (33)$$

and

$$\eta_{g,T} = \frac{dg_{\text{out}}^{(2)}(0)}{dT}. \quad (34)$$

The sensitivities $\eta_{n,T}$ and $\eta_{g,T}$ are plotted as functions of the temperature variation ΔT in Fig. 4(c). The maximal value of $\eta_{g,T}$ is about $28/^\circ\text{C}$, which is 3×10^3 times greater than the maximal values of $\eta_{n,T}$.

V. CONCLUSIONS

In conclusion, we have proposed schemes to realize sensitive sensing based on the correlation properties of mixing fields output from a MZI. We have demonstrated

that strong photon blockade can be achieved in the mixing field output from the two cavities in the two arms a MZI in the weak nonlinear regime. We also have proposed schemes to realize angular velocity and temperature sensing by measuring the second-order correlation of the photons output from the MZI, and shown that the strong photon blockade is much more sensitive to the parameters of system than the mean photon number. Our work opens a new way for sensitive sensing based on the quantum correlation of photons in the weak nonlinear regime.

ACKNOWLEDGMENTS

X.W.X. is supported by the National Natural Science Foundation of China (NSFC) (Grants No. 12064010, No. 12247105, and No. 12421005), the science and technology innovation Program of Hunan Province (Grant No. 2022RC1203), and Hunan provincial major sci-tech program (Grant No. 2023ZJ1010). H.J. is supported by the NSFC (Grant No. 11935006, 12421005), the Sci-Tech Innovation Program of Hunan Province (2020RC4047), the National Key R&D Program (2024YFE0102400), and the Hunan Major Sci-Tech Program (2023ZJ1010).

-
- [1] R. J. Glauber, Photon correlations, *Phys. Rev. Lett.* **10**, 84 (1963).
 - [2] R. J. Glauber, The quantum theory of optical coherence, *Phys. Rev.* **130**, 2529 (1963).
 - [3] S. Buckley, K. Rivoire, and J. Vučković, Engineered quantum dot single-photon sources, *Rep. Prog. Phys.* **75**, 126503 (2012).
 - [4] P. Lodahl, S. Mahmoodian, and S. Stobbe, Interfacing single photons and single quantum dots with photonic nanostructures, *Rev. Mod. Phys.* **87**, 347 (2015).
 - [5] S. Shi, B. Xu, K. Zhang, G.-S. Ye, D.-S. Xiang, Y. Liu, J. Wang, D. Su, and L. Li, High-fidelity photonic quantum logic gate based on near-optimal Rydberg single-photon source, *Nat. Commun.* **13**, 4454 (2022).
 - [6] M. Li, Y.-L. Zhang, H. X. Tang, C.-H. Dong, G.-C. Guo, and C.-L. Zou, Photon-photon quantum phase gate in a photonic molecule with $\chi^{(2)}$ nonlinearity, *Phys. Rev. Appl.* **13**, 044013 (2020).
 - [7] C. Wang, F.-M. Liu, M.-C. Chen, H. Chen, X.-H. Zhao, C. Ying, Z.-X. Shang, J.-W. Wang, Y.-H. Huo, C.-Z. Peng, X. Zhu, C.-Y. Lu, and J.-W. Pan, Realization of fractional quantum Hall state with interacting photons, *Science* **384**, 579 (2024).
 - [8] A. Imamoglu, H. Schmidt, G. Woods, and M. Deutsch, Strongly interacting photons in a nonlinear cavity, *Phys. Rev. Lett.* **79**, 1467 (1997).
 - [9] A. Ridolfo, M. Leib, S. Savasta, and M. J. Hartmann, Photon blockade in the ultrastrong coupling regime, *Phys. Rev. Lett.* **109**, 193602 (2012).
 - [10] Y.-x. Liu, X.-W. Xu, A. Miranowicz, and F. Nori, From blockade to transparency: Controllable photon transmission through a circuit-qed system, *Phys. Rev. A* **89**, 043818 (2014).
 - [11] A. Miranowicz, J. Bajer, M. Paprzycka, Y.-x. Liu, A. M. Zagoskin, and F. Nori, State-dependent photon blockade via quantum-reservoir engineering, *Phys. Rev. A* **90**, 033831 (2014).
 - [12] P. Rabl, Photon blockade effect in optomechanical systems, *Phys. Rev. Lett.* **107**, 063601 (2011).
 - [13] A. Nunnenkamp, K. Børkje, and S. M. Girvin, Single-photon optomechanics, *Phys. Rev. Lett.* **107**, 063602 (2011).
 - [14] J.-Q. Liao and F. Nori, Photon blockade in quadratically coupled optomechanical systems, *Phys. Rev. A* **88**, 023853 (2013).
 - [15] H. Xie, G.-W. Lin, X. Chen, Z.-H. Chen, and X.-M. Lin, Single-photon nonlinearities in a strongly driven optomechanical system with quadratic coupling, *Phys. Rev. A* **93**, 063860 (2016).
 - [16] A. Majumdar and D. Gerace, Single-photon blockade in doubly resonant nanocavities with second-order nonlinearity, *Phys. Rev. B* **87**, 235319 (2013).
 - [17] R. Huang, A. Miranowicz, J.-Q. Liao, F. Nori, and H. Jing, Nonreciprocal photon blockade, *Phys. Rev. Lett.* **121**, 153601 (2018).
 - [18] R. Huang, Ş. K. Özdemir, J.-Q. Liao, F. Minganti, L.-M. Kuang, F. Nori, and H. Jing, Exceptional Photon Blockade: Engineering Photon Blockade with Chiral Exceptional Points, *Laser Photon. Rev.* **16**, 2100430 (2022).
 - [19] S. Chakram, K. He, A. V. Dixit, A. E. Oriani, R. K. Naik, N. Leung, H. Kwon, W.-L. Ma, L. Jiang, and D. I. Schuster, Multimode photon blockade, *Nat. Phys.* **18**, 879 (2022).

- [20] Y. H. Zhou, X. Y. Zhang, Q. C. Wu, B. L. Ye, Z.-Q. Zhang, D. D. Zou, H. Z. Shen, and C.-P. Yang, Conventional photon blockade with a three-wave mixing, *Phys. Rev. A* **102**, 033713 (2020).
- [21] K. M. Birnbaum, A. Boca, R. Miller, A. D. Boozer, T. E. Northup, and H. J. Kimble, Photon blockade in an optical cavity with one trapped atom, *Nature (London)* **436**, 87 (2005).
- [22] B. Dayan, A. S. Parkins, T. Aoki, E. P. Ostby, K. J. Vahala, and H. J. Kimble, A Photon Turnstile Dynamically Regulated by One Atom, *Science* **319**, 1062 (2008).
- [23] T. Aoki, A. S. Parkins, D. J. Alton, C. A. Regal, B. Dayan, E. Ostby, K. J. Vahala, and H. J. Kimble, Efficient routing of single photons by one atom and a microtoroidal cavity, *Phys. Rev. Lett.* **102**, 083601 (2009).
- [24] A. Faraon, I. Fushman, D. Englund, N. Stoltz, P. Petroff, and J. Vučković, Coherent generation of non-classical light on a chip via photon-induced tunneling and blockade, *Nat. Phys.* **4**, 859 (2008).
- [25] A. Reinhard, T. Volz, M. Winger, A. Badolato, K. J. Hennessy, E. L. Hu, and A. Imamoglu, Strongly correlated photons on a chip, *Nature Photon.* **6**, 93 (2012).
- [26] C. Lang, D. Bozyigit, C. Eichler, L. Steffen, J. M. Fink, A. A. Abdumalikov, M. Baur, S. Filipp, M. P. da Silva, A. Blais, and A. Wallraff, Observation of resonant photon blockade at microwave frequencies using correlation function measurements, *Phys. Rev. Lett.* **106**, 243601 (2011).
- [27] A. J. Hoffman, S. J. Srinivasan, S. Schmidt, L. Spietz, J. Aumentado, H. E. Türeci, and A. A. Houck, Dispersive photon blockade in a superconducting circuit, *Phys. Rev. Lett.* **107**, 053602 (2011).
- [28] A. Lingenfelter, D. Roberts, and A. A. Clerk, Unconditional fock state generation using arbitrarily weak photonic nonlinearities, *Sci. Adv.* **7**, eabj1916 (2021).
- [29] Y.-X. Ma and P.-B. Li, Deterministic generation of phononic fock states via weak nonlinearities, *Phys. Rev. A* **108**, 053709 (2023).
- [30] Y.-H. Zhou, X.-Y. Zhang, T. Liu, Q.-C. Wu, Z.-C. Shi, H.-Z. Shen, and C.-P. Yang, Environmentally induced photon blockade via two-photon absorption, *Phys. Rev. Appl.* **18**, 064009 (2022).
- [31] X. Su, J.-S. Tang, and K. Xia, Nonlinear dissipation-induced photon blockade, *Phys. Rev. A* **106**, 063707 (2022).
- [32] A. Ben-Asher, A. I. Fernández-Domínguez, and J. Feist, Non-Hermitian Anharmonicity Induces Single-Photon Emission, *Phys. Rev. Lett.* **130**, 243601 (2023).
- [33] Y. Zuo, R. Huang, L.-M. Kuang, X.-W. Xu, and H. Jing, Loss-induced suppression, revival, and switch of photon blockade, *Phys. Rev. A* **106**, 043715 (2022).
- [34] G. Y. Kryuchkyan, A. R. Shahinyan, and I. A. Shelykh, Quantum statistics in a time-modulated exciton-photon system, *Phys. Rev. A* **93**, 043857 (2016).
- [35] G. H. Hovsepyan, A. R. Shahinyan, and G. Y. Kryuchkyan, Multiphoton blockades in pulsed regimes beyond stationary limits, *Phys. Rev. A* **90**, 013839 (2014).
- [36] O. Kyriienko and T. C. H. Liew, Triggered single-photon emitters based on stimulated parametric scattering in weakly nonlinear systems, *Phys. Rev. A* **90**, 063805 (2014).
- [37] S. Ghosh and T. C. H. Liew, Single photons from a gain medium below threshold, *Phys. Rev. B* **97**, 241301 (2018).
- [38] S. Ghosh and T. C. H. Liew, Dynamical blockade in a single-mode bosonic system, *Phys. Rev. Lett.* **123**, 013602 (2019).
- [39] M. Li, Y.-L. Zhang, S.-H. Wu, C.-H. Dong, X.-B. Zou, G.-C. Guo, and C.-L. Zou, Single-mode photon blockade enhanced by bi-tone drive, *Phys. Rev. Lett.* **129**, 043601 (2022).
- [40] D. Stefanatos and E. Paspalakis, Dynamical blockade in a bosonic Josephson junction using optimal coupling, *Phys. Rev. A* **102**, 013716 (2020).
- [41] T. C. H. Liew and V. Savona, Single photons from coupled quantum modes, *Phys. Rev. Lett.* **104**, 183601 (2010).
- [42] M. Bamba, A. Imamoglu, I. Carusotto, and C. Ciuti, Origin of strong photon antibunching in weakly nonlinear photonic molecules, *Phys. Rev. A* **83**, 021802 (2011).
- [43] X.-W. Xu and Y.-J. Li, Antibunching photons in a cavity coupled to an optomechanical system, *J. Phys. B: At. Mol. Opt. Phys.* **46**, 035502 (2013).
- [44] V. Savona, Unconventional photon blockade in coupled optomechanical systems, [arXiv:1302.5937](https://arxiv.org/abs/1302.5937).
- [45] W.-Z. Zhang, J. Cheng, J.-Y. Liu, and L. Zhou, Controlling photon transport in the single-photon weak-coupling regime of cavity optomechanics, *Phys. Rev. A* **91**, 063836 (2015).
- [46] S. Ferretti, V. Savona, and D. Gerace, Optimal antibunching in passive photonic devices based on coupled nonlinear resonators, *New J. Phys.* **15**, 025012 (2013).
- [47] H. Flayac and V. Savona, Input-output theory of the unconventional photon blockade, *Phys. Rev. A* **88**, 033836 (2013).
- [48] D. Gerace and V. Savona, Unconventional photon blockade in doubly resonant microcavities with second-order nonlinearity, *Phys. Rev. A* **89**, 031803 (2014).
- [49] X.-W. Xu and Y. Li, Tunable photon statistics in weakly nonlinear photonic molecules, *Phys. Rev. A* **90**, 043822 (2014).
- [50] X.-W. Xu and Y. Li, Strong photon antibunching of symmetric and antisymmetric modes in weakly nonlinear photonic molecules, *Phys. Rev. A* **90**, 033809 (2014).
- [51] M.-A. Lemonde, N. Didier, and A. A. Clerk, Antibunching and unconventional photon blockade with Gaussian squeezed states, *Phys. Rev. A* **90**, 063824 (2014).
- [52] H. Z. Shen, Y. H. Zhou, and X. X. Yi, Tunable photon blockade in coupled semiconductor cavities, *Phys. Rev. A* **91**, 063808 (2015).
- [53] Y. H. Zhou, H. Z. Shen, and X. X. Yi, Unconventional photon blockade with second-order nonlinearity, *Phys. Rev. A* **92**, 023838 (2015).
- [54] H. Flayac and V. Savona, Unconventional photon blockade, *Phys. Rev. A* **96**, 053810 (2017).
- [55] B. Sarma and A. K. Sarma, Quantum-interference-assisted photon blockade in a cavity via parametric interactions, *Phys. Rev. A* **96**, 053827 (2017).
- [56] Y. H. Zhou, F. Minganti, W. Qin, Q.-C. Wu, J.-L. Zhao, Y.-L. Fang, F. Nori, and C.-P. Yang, n -photon blockade with an n -photon parametric drive, *Phys. Rev. A* **104**, 053718 (2021).
- [57] S. Shen, Y. Qu, J. Li, and Y. Wu, Tunable photon statistics in parametrically amplified photonic molecules, *Phys. Rev. A* **100**, 023814 (2019).
- [58] E. Zubizarreta Casalengua, J. C. López Carreño, F. P. Laussy, and E. del Valle, Conventional and unconven-

- tional photon statistics, *Laser Photon. Rev.* **14**, 1900279 (2020).
- [59] E. Zubizarreta Casalengua, J. C. López Carreño, F. P. Laussy, and E. del Valle, Tuning photon statistics with coherent fields, *Phys. Rev. A* **101**, 063824 (2020).
- [60] D.-Y. Wang, C.-H. Bai, S. Liu, S. Zhang, and H.-F. Wang, Photon blockade in a double-cavity optomechanical system with nonreciprocal coupling, *New J. Phys.* **22**, 093006 (2020).
- [61] A. Majumdar, M. Bajcsy, A. Rundquist, and J. Vučković, Loss-enabled sub-poissonian light generation in a bimodal nanocavity, *Phys. Rev. Lett.* **108**, 183601 (2012).
- [62] W. Zhang, Z. Yu, Y. Liu, and Y. Peng, Optimal photon antibunching in a quantum-dot-bimodal-cavity system, *Phys. Rev. A* **89**, 043832 (2014).
- [63] J. Tang, W. Geng, and X. Xu, Quantum Interference Induced Photon Blockade in a Coupled Single Quantum Dot-Cavity System, *Sci. Rep.* **5**, 9252 (2015).
- [64] X. Liang, Z. Duan, Q. Guo, C. Liu, S. Guan, and Y. Ren, Antibunching effect of photons in a two-level emitter-cavity system, *Phys. Rev. A* **100**, 063834 (2019).
- [65] O. Kyriienko, D. N. Krizhanovskii, and I. A. Shelykh, Nonlinear Quantum Optics with Trion Polaritons in 2D Monolayers: Conventional and Unconventional Photon Blockade, *Phys. Rev. Lett.* **125**, 197402 (2020).
- [66] Y. Wang, W. Verstraelen, B. Zhang, T. C. H. Liew, and Y. D. Chong, Giant enhancement of unconventional photon blockade in a dimer chain, *Phys. Rev. Lett.* **127**, 240402 (2021).
- [67] J. Li, C.-M. Hu, and Y. Yang, Enhancement of photon blockade via topological edge states, *Phys. Rev. Appl.* **21**, 034058 (2024).
- [68] Z.-G. Lu, Y. Wu, and X.-Y. Lü, Chiral interaction induced near-perfect photon blockade, [arXiv:2402.09000](https://arxiv.org/abs/2402.09000).
- [69] H. J. Snijders, J. A. Frey, J. Norman, H. Flayac, V. Savona, A. C. Gossard, J. E. Bowers, M. P. van Exter, D. Bouwmeester, and W. Löffler, Observation of the unconventional photon blockade, *Phys. Rev. Lett.* **121**, 043601 (2018).
- [70] C. Vaneph, A. Morvan, G. Aiello, M. Féchant, M. Aprili, J. Gabelli, and J. Estève, Observation of the unconventional photon blockade in the microwave domain, *Phys. Rev. Lett.* **121**, 043602 (2018).
- [71] Z.-H. Liu and X.-W. Xu, Scaling enhancement of photon blockade in output fields, [arXiv:2403.18299](https://arxiv.org/abs/2403.18299).
- [72] M. Born and E. Wolf, *Principles of Optics: 60th Anniversary Edition*, 7th ed. (Cambridge University Press, 2019).
- [73] M. Terrel, M. J. F. Digonnet, and S. Fan, Ring-coupled Mach-Zehnder interferometer optimized for sensing, *Appl. Opt.* **48**, 4874 (2009).
- [74] P. P. Khial, A. D. White, and A. Hajimiri, Nanophotonic optical gyroscope with reciprocal sensitivity enhancement, *Nature Photon.* **12**, 671 (2018).
- [75] Y. Zhao, H. Zhao, R.-q. Lv, and J. Zhao, Review of optical fiber Mach-Zehnder interferometers with microcavity fabricated by femtosecond laser and sensing applications, *Opt. Lasers Eng.* **117**, 7 (2019).
- [76] W. W. Chow, J. Gea-Banacloche, L. M. Pedrotti, V. E. Sanders, W. Schleich, and M. O. Scully, The ring laser gyro, *Rev. Mod. Phys.* **57**, 61 (1985).
- [77] G. E. Stedman, Ring-laser tests of fundamental physics and geophysics, *Rep. Prog. Phys.* **60**, 615 (1997).
- [78] R. Li, W. Fan, L. Jiang, L. Duan, W. Quan, and J. Fang, Rotation sensing using a K-Rb-²¹Ne comagnetometer, *Phys. Rev. A* **94**, 032109 (2016).
- [79] J. Ren, H. Hodaei, G. Harari, A. U. Hassan, W. Chow, M. Soltani, D. Christodoulides, and M. Khajavikhan, Ultrasensitive micro-scale parity-time-symmetric ring laser gyroscope, *Opt. Lett.* **42**, 1556 (2017).
- [80] J. Li, M.-G. Suh, and K. Vahala, Microresonator Brillouin gyroscope, *Optica* **4**, 346 (2017).
- [81] S. Sunada, Large sagnac frequency splitting in a ring resonator operating at an exceptional point, *Phys. Rev. A* **96**, 033842 (2017).
- [82] K. Li, S. Davuluri, and Y. Li, Improving optomechanical gyroscopes by coherent quantum noise cancellation processing, *Sci. China Phys. Mech. Astron.* **61**, 90311 (2018).
- [83] M. D. Carlo, F. D. Leonardis, L. Lamberti, and V. M. N. Passaro, High-sensitivity real-splitting anti-PT-symmetric microscale optical gyroscope, *Opt. Lett.* **44**, 3956 (2019).
- [84] Y.-H. Lai, Y.-K. Lu, M.-G. Suh, Z. Yuan, and K. Vahala, Observation of the exceptional-point-enhanced Sagnac effect, *Nature (London)* **576**, 65 (2019).
- [85] M. P. Hokmabadi, A. Schumer, D. N. Christodoulides, and M. Khajavikhan, Non-Hermitian ring laser gyroscopes with enhanced Sagnac sensitivity, *Nature (London)* **576**, 70 (2019).
- [86] X. Mao, G.-Q. Qin, H. Yang, H. Zhang, M. Wang, and G.-L. Long, Enhanced sensitivity of optical gyroscope in a mechanical parity-time-symmetric system based on exceptional point, *New J. Phys.* **22**, 093009 (2020).
- [87] H. Zhang, M. Peng, X.-W. Xu, and H. Jing, Anti-PT-symmetric Kerr gyroscope, *Chinese Phys. B* **31**, 014215 (2022).
- [88] F. Giazotto, T. T. Heikkilä, A. Luukanen, A. M. Savin, and J. P. Pekola, Opportunities for mesoscopics in thermometry and refrigeration: Physics and applications, *Rev. Mod. Phys.* **78**, 217 (2006).
- [89] S. Dedyulin, Z. Ahmed, and G. Machin, Emerging technologies in the field of thermometry, *Meas. Sci. Technol.* **33**, 092001 (2022).
- [90] E. Moreva, E. Bernardi, P. Traina, A. Sosso, S. D. Tchernij, J. Forneris, F. Picollo, G. Brida, Ž. Pastuović, I. P. Degiovanni, P. Olivero, and M. Genovese, Practical applications of quantum sensing: A simple method to enhance the sensitivity of nitrogen-vacancy-based temperature sensors, *Phys. Rev. Appl.* **13**, 054057 (2020).
- [91] H. Xu, M. Hafezi, J. Fan, J. M. Taylor, G. F. Strouse, and Z. Ahmed, Ultra-sensitive chip-based photonic temperature sensor using ring resonator structures, *Opt. Express* **22**, 3098 (2014).
- [92] N. Klimov, T. Purdy, and Z. Ahmed, Towards replacing resistance thermometry with photonic thermometry, *Sensors and Actuators A: Physical* **269**, 308 (2018).
- [93] J. Liao and L. Yang, Optical whispering-gallery mode barcodes for high-precision and wide-range temperature measurements, *Light Sci. Appl.* **10**, 32 (2021).
- [94] C.-H. Dong, L. He, Y.-F. Xiao, V. R. Gaddam, S. K. Ozdemir, Z.-F. Han, G.-C. Guo, and L. Yang, Fabrication of high-Q polydimethylsiloxane optical microspheres for thermal sensing, *Appl. Phys. Lett.* **94**, 231119 (2009).

- [95] B.-B. Li, Q.-Y. Wang, Y.-F. Xiao, X.-F. Jiang, Y. Li, L. Xiao, and Q. Gong, On chip, high-sensitivity thermal sensor based on high-Q polydimethylsiloxane-coated microresonator, *Appl. Phys. Lett.* **96**, 251109 (2010).
- [96] D. Xie and C. Xu, Thermometry with a dissipative heavy impurity, *Phys. Rev. Res.* **6**, 033102 (2024).
- [97] T. P. Purdy, P.-L. Yu, N. S. Kampel, R. W. Peterson, K. Cicak, R. W. Simmonds, and C. A. Regal, Optomechanical Raman-ratio thermometry, *Phys. Rev. A* **92**, 031802 (2015).
- [98] Q. Wang, J.-Q. Zhang, P.-C. Ma, C.-M. Yao, and M. Feng, Precision measurement of the environmental temperature by tunable double optomechanically induced transparency with a squeezed field, *Phys. Rev. A* **91**, 063827 (2015).
- [99] T. P. Purdy, K. E. Grutter, K. Srinivasan, and J. M. Taylor, Quantum correlations from a room-temperature optomechanical cavity, *Science* **356**, 1265 (2017).
- [100] A. Chowdhury, P. Vezio, M. Bonaldi, A. Borrielli, F. Marino, B. Morana, G. Pandraud, A. Pontin, G. A. Prodi, P. M. Sarro, E. Serra, and F. Marin, Calibrated quantum thermometry in cavity optomechanics, *Quantum Sci. Technol.* **4**, 024007 (2019).
- [101] V. Montenegro, M. G. Genoni, A. Bayat, and M. G. A. Paris, Mechanical oscillator thermometry in the nonlinear optomechanical regime, *Phys. Rev. Research* **2**, 043338 (2020).
- [102] I. Galinskiy, Y. Tsaturyan, M. Parniak, and E. S. Polzik, Phonon counting thermometry of an ultracoherent membrane resonator near its motional ground state, *Optica* **7**, 718 (2020).
- [103] R. Singh and T. P. Purdy, Detecting acoustic blackbody radiation with an optomechanical antenna, *Phys. Rev. Lett.* **125**, 120603 (2020).
- [104] M. Shirzad, R. Rognizadeh, and A. Mahdifar, Exploring the feasibility of optomechanical systems for temperature estimation in interferometric setups, *Phys. Rev. A* **109**, 053509 (2024).
- [105] M. Mehboudi, A. Sanpera, and L. A. Correa, Thermometry in the quantum regime: recent theoretical progress, *J. Phys. A: Math. Theor.* **52**, 303001 (2019).
- [106] C. Potts, V. Bittencourt, S. V. Kusminskiy, and J. Davis, Magnon-phonon quantum correlation thermometry, *Phys. Rev. Applied* **13**, 064001 (2020).
- [107] W.-K. Mok, K. Bharti, L.-C. Kwek, and A. Bayat, Optimal probes for global quantum thermometry, *Commun. Phys.* **4**, 62 (2021).
- [108] N. Zhang, C. Chen, S.-Y. Bai, W. Wu, and J.-H. An, Non-Markovian Quantum Thermometry, *Phys. Rev. Appl.* **17**, 034073 (2022).
- [109] J.-B. Yuan, B. Zhang, Y.-J. Song, S.-Q. Tang, X.-W. Wang, and L.-M. Kuang, Quantum sensing of temperature close to absolute zero in a Bose-Einstein condensate, *Phys. Rev. A* **107**, 063317 (2023).
- [110] L. Xu, J.-B. Yuan, S.-Q. Tang, W. Wu, Q.-S. Tan, and L.-M. Kuang, Non-Markovian enhanced temperature sensing in a dipolar Bose-Einstein condensate, *Phys. Rev. A* **108**, 022608 (2023).
- [111] Y. Aiache, C. Seida, K. El Anouz, and A. El Allati, Non-Markovian enhancement of nonequilibrium quantum thermometry, *Phys. Rev. E* **110**, 024132 (2024).
- [112] N. Zhang, S.-Y. Bai, and C. Chen, Temperature-heat uncertainty relation in nonequilibrium quantum thermometry, *Phys. Rev. A* **110**, 012211 (2024).
- [113] Y. Aiache, A. El Allati, and K. El Anouz, Harnessing coherence generation for precision single- and two-qubit quantum thermometry, *Phys. Rev. A* **110**, 032605 (2024).
- [114] D.-J. Zhang and D. M. Tong, Approaching Heisenberg-scalable thermometry with built-in robustness against noise, *npj Quantum Inf.* **8**, 81 (2022).
- [115] V. Mukherjee, A. Zwick, A. Ghosh, X. Chen, and G. Kurizki, Enhanced precision bound of low-temperature quantum thermometry via dynamical control, *Commun. Phys.* **2**, 162 (2019).
- [116] C. W. Gardiner and M. J. Collett, Input and output in damped quantum systems: Quantum stochastic differential equations and the master equation, *Phys. Rev. A* **31**, 3761 (1985).
- [117] H. Carmichael, *An Open Systems Approach to Quantum Optics* (Springer-Verlag Berlin Heidelberg, 1993).
- [118] B. Culshaw, The optical fibre sagnac interferometer: an overview of its principles and applications, *Meas. Sci. Technol.* **17**, R1 (2005).
- [119] M. Cavillon, P. D. Dragic, and J. Ballato, Additivity of the coefficient of thermal expansion in silicate optical fibers, *Opt. Lett.* **42**, 3650 (2017).
- [120] H. Gao, Y. Jiang, Y. Cui, L. Zhang, J. Jia, and L. Jiang, Investigation on the thermo-optic coefficient of silica fiber within a wide temperature range, *J. Lightwave Technol.* **36**, 5881 (2018).